Potentiostatic step experiments on pasted Pb–Sb and Pb–Sn–Ca electrodes

J. A. BIALACKI, N. A. HAMPSON

Chemistry Department, University of Technology, Loughborough, Leics. LE11 3TU, UK

F. WILSON

Chloride Technical Ltd, Wynne Avenue, Swinton, Manchester M27 2HB, UK

A range of cyclic electrochemical experiments have been carried out on electrodes of porous PbO_2 supported on a number of Pb–Sb and Pb–Sn–Ca alloys using micro-computer controlled potentiostatic stepping techniques. The results show that, in certain cases, the differences in electrochemical behaviour of the PbO_2 can be interpreted as being due to the effect of the support alloy.

1. Introduction

Antimony has for a long time been used as an alloying ingredient in the support grid of the lead acid positive electrode. It was originally added to strengthen and stiffen the base lead; however, in recent years the industry has come to recognize that other beneficial effects were conferred on the performance and life of the positive active material. A disadvantage of antimony is that it is slowly leached from the lead alloy and deposited on the negative plate thereby reducing the hydrogen overvoltage at this electrode.

The search for antimony substitutes has identified Pb–Sn–Ca alloys of appropriate mechanical properties as being completely free from hydrogen evolution effects. It appears that maintenance-free battery units requiring only a very small overvoltage in order to offset internal self-discharge can be perfected for stand-by applications. Fully sealed automotive batteries with minimal capacity loss due to self-discharge and negligible water loss in service have recently reached the commercial market. Both these applications rely on the desirable properties of the Pb–Sn–Ca alloy.

During the last decade in which these developments have been taking place, it has been realized that positive electrodes prepared on antimony-free grids were inferior in both cycle life span and performance after cycling duty. This shortcoming

appeared to be a positive effect of antimony on that of the basic pure lead rather than a detrimental effect of tin and calcium on the basic behaviour. There was also considerable industrial evidence that the grid effects (as they ought to be called) were dependent on the amount and character of the cycling to which the electrodes were subjected; a newly formed positive electrode exhibits a behaviour independent of the grid whereas as few as 10 cycles would show up gross differences in behaviour.

With the present intense interest in the fully-sealed low-loss battery it was considered important to identify the specific grid effects attributable to the alloys Pb–Sb and Pb–Sn–Ca of the relevant commercial compositions. In this paper we present the results of such an investigation in which we have investigated specific effects as functions of cycle number.

2. Experimental method

The electrochemical stepping experiments were performed using a micro-computer as described by Mitchell [1] controlling a potentiostat (Kemitron POT.03); the data obtained from the pulse experiments were captured by a transient recorder (Datalab, DL 905) which in turn transferred back to the computer. An oscilloscope (Hameg HM 512) was used to display the data recorded by the transient recorder.

The electrodes in which a porous PbO_2 phase (derived from a conventional battery paste) overlays the desired base alloy shrouded in Teflon and forming the working face of an RDE electrode have already been described [2]. The initial oxidation of paste to PbO_2 was carried out and has also been described [2]. When formed, the working porous electrode was a cylinder (0.07 cm^2 area, 0.076 cm deep; of equivalent electrical charge ~ 16 C).

The base lead alloys used for the porous PbO_2 supports were:

Code	Analysis (wt %)			
	Sb	Ca	Sn	Pb
A	–	–	–	99.999
B	0.58	–	–	Remainder
C	1.88	–	–	Remainder
D	4.18	–	–	Remainder
E	–	0.086	0.34	Remainder
F	–	0.076	0.75	Remainder

The composition of the paste used was as follows:

Grey oxide	85.7%
Red lead	14.3%
1.4 s.g. H_2SO_4	53.49 cm^3 kg^{-1}
H_2O	123.57 cm^3 kg^{-1}

3. Results and discussion

3.1. Uncycled electrodes

Fig. 1 shows the current–time responses of the porous antimonial–lead electrodes (compared with a pasted pure lead electrode) as the potential* is instantaneously stepped from the lead dioxide region (1240 mV) to the lead sulphate region (700 mV). As can be seen, B, which contains the least amount of antimony, discharges very quickly and gives the highest current output, that is, $i_{max} = 140$ mA. The low Sb content probably gives rise to more β-PbO_2 being produced compared to α-PbO_2. Burbank et al. [3] have suggested that in a mixture of the two polymorphs

---

* An Hg/Hg_2SO_4 reference electrode was used throughout and all potentials are quoted on this scale ($23 \pm 1^\circ$ C).
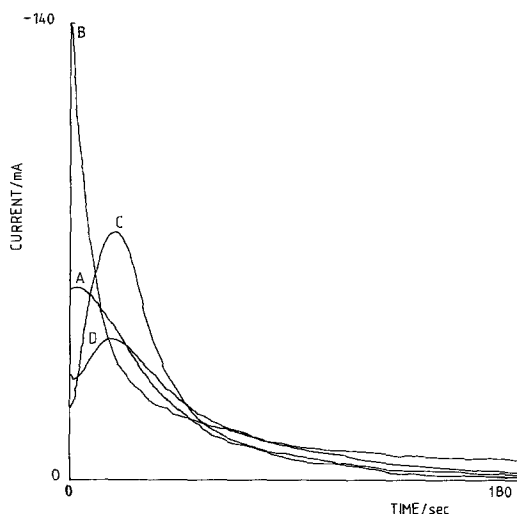

Fig. 1. Potentiostatic pulse experiments from 1240 to 700 mV on formed pasted electrodes on Pb and Pb–Sb bases. Letters refer to electrodes described in Section 2.

α-PbO_2 and β-PbO_2 the β-PbO_2 contributes more to the electrochemical capacity of the positive battery plate. Consequently, the higher the Sb content, the less β-PbO_2 is formed on galvanostatic oxidation and hence a lower peak current output is obtained. The pure Pb electrode A gives an appreciable amount of β-PbO_2, intermediate in quantity between the contents of C and D. This results in an i_{max} which lies between the values obtained with C and D. It may be that the particular i_{max} value obtained for pure lead is a result of enhanced acid availability at the reaction site due in some way to the greater resistance to oxidative corrosion of pure Pb vis à vis antimonial lead. In Fig. 1 only the D electrode shows signs of another reaction occurring which is represented by the initial dip before the peak.

The electrodes were then stepped back into the lead dioxide region (1240 mV) from the fully reduced state. Fig. 2 displays the current–time responses as the electrodes were subjected to this oxidation. The initial double layer charging spike is followed by an increase in the current due to the formation and growth of nucleation centres. The following decrease in the current flow is the result of subsequent overlap of these growth centres. However, the peaks are followed by constant current outputs over a fairly long time period, especially with electrodes B and C. This indicates
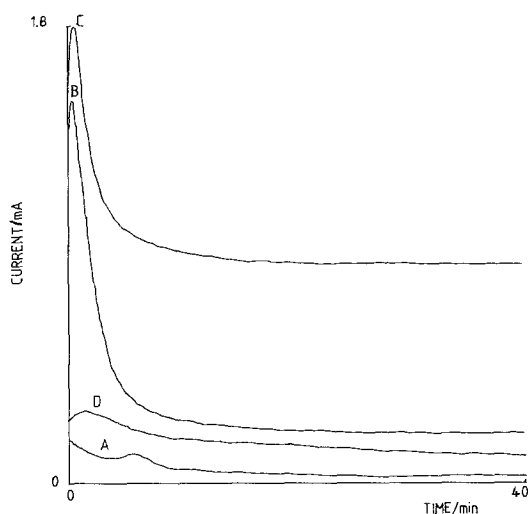
Fig. 2. Potentiostatic pulse experiments from 700 to 1240 mV on the electrodes used in Fig. 1 following full discharge.

Table 1. Capacities for the porous electrodes subjected to potentiostatic reduction followed by oxidation

Alloys	Discharge capacity (C)	Time to reach full discharge capacity (min)	Recharge capacity after 4 h (C)
A	11.54	150	0.97
B	8.52	180	1.21
C	7.55	145	0.78
D	10.50	210	0.66
E	7.87	150	1.12
F	4.53	85	1.67

that the current flow is partly due to oxygen evolution since the lead dioxide and oxygen regions overlap. The D electrode accepts less charge than the other two pasted antimonial–lead electrodes. This result is interesting in view of that obtained by Kelly et al. [2] and it should be noted that the potential step used here was different, in our case 700–1240 mV, and the paste employed had a density of 4.2 g cm^{-3}. Kelly et al. used a paste which contained 100% grey oxide and was of density 4.1 g cm^{-3}.
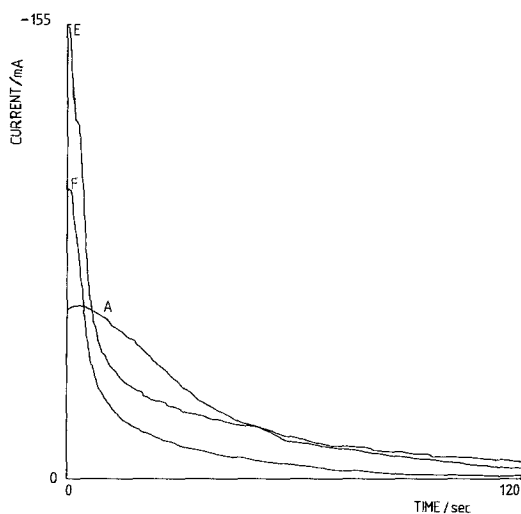
Fig. 3 shows the current–time responses of the porous PbO_2 electrodes on Pb–Sn–Ca bases corresponding to a potentiostatic reduction pulse of the same magnitude as with the Pb–Sb based electrodes. E has the highest i_{max} value compared with the other five positives. However, Table 1 shows that the discharge capacity of E is less than that obtained with A, B and D. Fig. 4 shows the current–time responses for the porous PbO_2 electrodes on Pb–Sn–Ca bases after each one was oxidized potentiostatically by stepping from 700 to 1240 mV. It seems unusual that electrode F accepts more charge (700 → 1240 mV) than the other electrodes since it discharges the least (1240 → 700 mV). Also the resultant curve

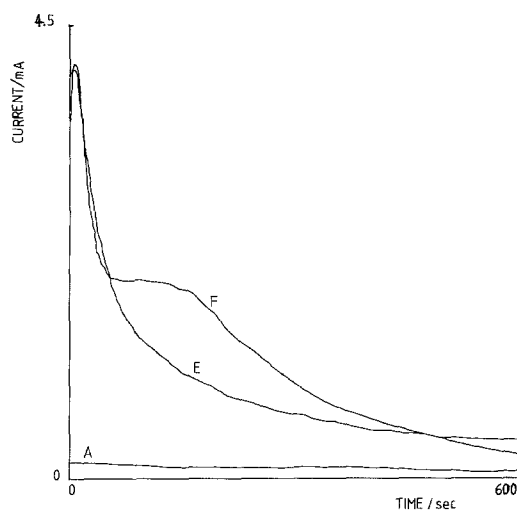Fig. 3. The same conditions as in Fig. 1 but using Pb and Pb–Sn–Ca based porous electrodes.

Fig. 4. Potentiostatic pulse experiments from 700 to 1240 mV on the electrodes in Fig. 3 following full discharge.

obtained for F suggests that another layer of PbO$_2$ has been formed.

All the pasted alloy electrodes investigated exhibited a very slow (i.e. low current) charge acceptance as can be seen from Table 1 which shows oxidation current still flowing after 4 h. Kelly *et al.* [2] considered that this effect was due to the reluctance of certain crystals of lead sulphate ('passive' PbSO$_4$) to oxidize to lead dioxide. The electrode is never fully charged potentiostatting at 1240 mV and thus a higher potential is required to fully form PbO$_2$. Hence, before each experiment the electrode was galvano-statically oxidized [2] to ensure that it was fully charged. Figs. 2 and 4 show that the magnitude of the peak currents for the Pb–Sn–Ca based electrodes are higher than those for the Pb–Sb positives. Also, Table 1 shows there is an imbalance between reductive and oxidative charge with all the electrodes. This imbalance remaining after 4 h reoxidation was investigated in the cases of C and E, which were of special interest, using scanning electron microscopy (SEM) and X-ray diffraction [4]. It was found that there were clear unambiguous evidence for PbSO$_4$ crystals remaining amongst the PbO$_2$. These crystals are the inactive PbSO$_4$, as mentioned earlier. The absence of such crystals on the completion of the galvanostatic oxidation was confirmed immediately before the reduction by direct examination of the electrodes by SEM. Morphological examination of the electrodes C and E after potentiostatically oxidizing for 4 h at 1240 mV showed that the Pb–Sn–Ca positive contained a high proportion of β-PbO$_2$ whereas the Pb–Sb positive contained a high proportion of α-PbO$_2$. It seems that the better charge acceptance of the Pb–Sn–Ca electrode is

Fig. 6. ln i vs $t^{0.5}$ for falling part in Fig. 3 for uncycled alloy E based 'positive'.

a result of the higher proportion of the β-polymorph in the final electrode state. However, this is not conclusive.

A number of established current–time relationships for electrocrystallization processes [5] were used to match the falling parts of the transients in Figs. 1–4. Using the Least Squares Fit method, via the on-line computer, a variety of straight line plots were obtained and the 'best' straight line identified by the correlation coefficient. From the data of Figs. 1 and 3 it was found that all the electrodes followed a ln i vs $t^{1/2}$ relationship as typified in Figs. 5 and 6 for electrodes C and E, respectively.

3.2. *Cycled electrodes*

3.2.1. *Electrodes subjected to twenty preparatory cycles.* Before potentiostatic stepping experiments the porous electrodes were subjected to a series of cycles using (digital) linear sweep voltammetry. Freshly prepared electrodes were cycled for 20 cycles of discharge and charge from 1240 to 700 mV at 10 mV s^{-1} and back again; the step

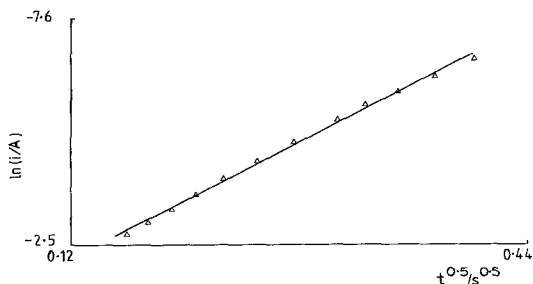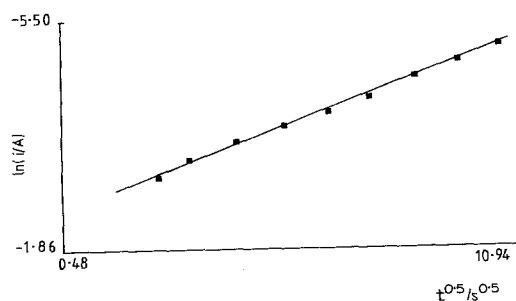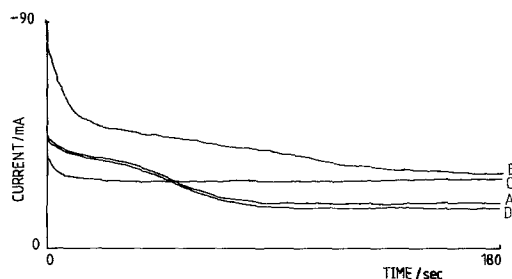

Fig. 5. ln i vs $t^{0.5}$ for falling part in Fig. 1 for uncycled formed and pasted (PbO$_2$) 'positive' porous electrode on alloy C.

Fig. 7. Current–time transients for potentiostatic pulse experiments (1240–700 mV) on cycled (20 cycles) Pb and Pb–Sb based porous electrodes.
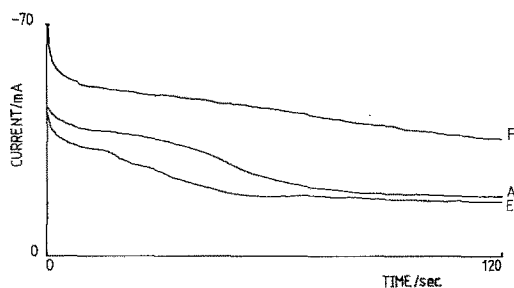
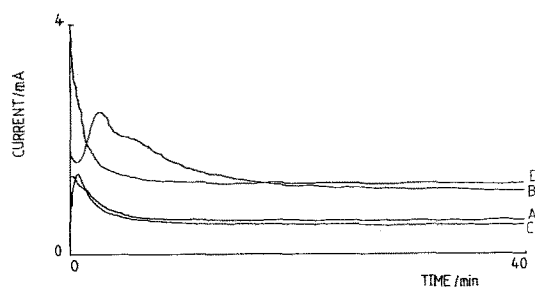Fig. 8. As in Fig. 7, but for Pb and Pb–Sn–Ca based porous electrodes.

Fig. 9. Current–time transients for potentiostatic pulse experiments (700–1240 mV) on cycled (20 cycles) Pb and Pb–Sb based porous electrodes, following a full discharge.

experiment is therefore to be performed on a pre-conditioned electrode containing an 'equilibrium' amount of $PbSO_4$ arising from the out-of-balance of the extents of the oxidation/reduction processes under these conditions. (Before a pulse was performed, care was taken to ensure that the electrode was in a steady state at 1240 mV, that is, the current output was low (1 μA) and constant.) After cycling a potentiostatic reduction pulse (1240 → 700 mV) was then performed. Figs. 7 and 8 show the current–time responses for the porous electrodes corresponding to the potentiostatic reduction. The peak current output decreases as a consequence of the cycling process. Table 2 shows that the discharge capacities of the electrodes, as well as the times taken, are lower compared with those values corresponding to the un-cycled electrodes. The decrease in the discharge capacity with cycling is apparently due to the production of inactive lead sulphate [2] during the preparatory linear sweep voltammetry since no lead material was observed to leave the electrode. The conclusion is that on the anodic sweep of the cycle relatively inactive lead sulphate

crystals remain unoxidized reducing the amount of PbO_2 available for subsequent reduction in the potentiostatic reaction.

With continued redox cycling the capacities of all the electrodes, judged by the peak current output, on reduction were reduced. In Figs. 7 and 8 the curvature of the transients are somewhat reduced probably because some 'passivated' lead sulphate has already been formed during cycling, so that less PbO_2 is present before the potentiostatic reduction pulse to $PbSO_4$.

Figs. 9 and 10 show the current–time responses of the porous electrodes after 20 cycles of linear sweep voltammetry and stepping from the lead sulphate region to the lead dioxide region after fully discharging. The peak current output has increased compared with the uncycled pasted electrodes although the charge acceptance after 4 h is less. (See Tables 1 and 2.) As can be seen the alloy D electrode (with the highest antimony content) has the highest peak current output compared with the other pasted Pb–Sb electrodes. With the alloy B electrode more than one process is occurring as a consequence of the potential
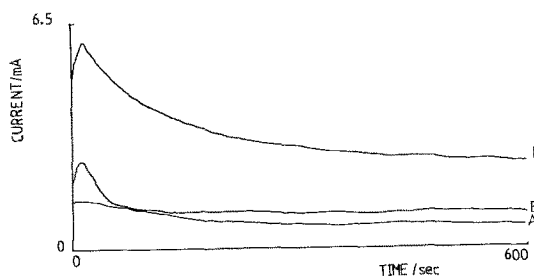
Table 2. As Table 1 but for cycled (20 cycles) porous electrodes

Alloys	Discharge capacity (C)	Time to reach full discharge capacity (min)	Recharge capacity after 4 h (C)
A	3.52	40	0.24
B	2.88	30	0.43
C	2.30	5	0.61
D	2.46	15	0.33
E	2.96	10	0.72
F	0.77	30	0.25

Fig. 10. As in Fig. 9, but for Pb and Pb–Sn–Ca based porous electrodes, following a complete discharge.
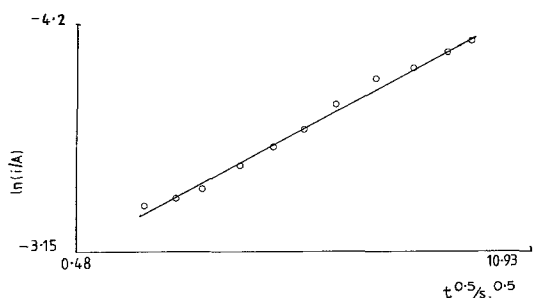
Fig. 11. ln i vs $t^{0.5}$ for falling part in Fig. 8 for cycled (20 cycles) alloy E based porous electrode.

Fig. 13. Potentiostatic pulse experiments from 1240 to 700 mV on alloy C based porous electrode following a series of cycles.

step to PbO_2 (1240 mV), hence possibly a more porous form of PbO_2 structure is being produced. Fig. 10 shows that alloy F electrode has a higher peak current output than the alloy E electrode. However, Table 2 highlights the fact that electrode E accepts more charge than the other electrodes. It is less than the corresponding value obtained in the uncycled condition. Also, the intermediate Sb content electrode (C) accepts more charge than the other two Pb–Sb positives. As yet no reason can be found to explain these results.

Again, using the Least Squares Fit method, for the falling parts of the transients in Figs. 7–10, the porous electrodes, except alloy C, after a reductive pulse (1240 → 700 mV), follow a ln i vs $t^{1/2}$ relationship, Fig. 11 being an example for the electrode E. Electrode C, however, when subjected to a reductive pulse followed a process for which $i \propto t^{-1/2}$, as shown in Fig. 12. This agrees with Dawson et al. [6] who found that the discharge of β-lead dioxide occurs by two mechanisms: a diffusion controlled outer layer discharge by a dissolution–precipitation mechanism i vs $t^{-1/2}$. Within the pores of the growing $PbSO_4$
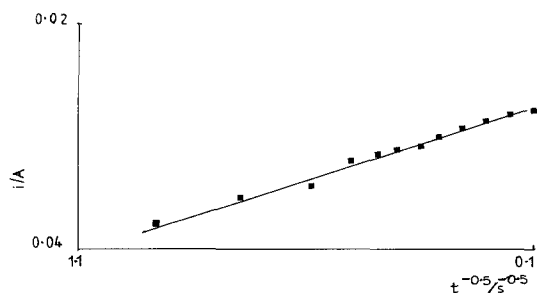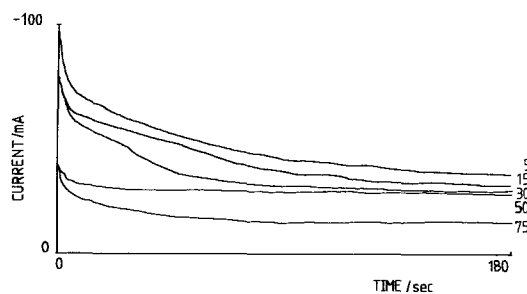
layer diffusion occurs together with an electrocrystallization reaction of the inner layer of PbO_2, and under certain conditions, a solid state electrocrystallization process of i vs t^2 occurs when PbO_2 reduces to PbO and $PbSO_4$.

3.2.2. Variation in number of preparatory cycles.
A number of experiments were made in order to explain the variation of current output with cycling. Electrodes C and E, of considerable industrial importance, were used. The electrodes were initially galvanostatically oxidized [2] to ensure that a fully recharged state had been obtained followed by a reductive pulse (1240 → 700 mV). Figs. 13 and 14 show the results. The peak current output decreases with the number of linear sweep cycles. This is to be expected following the work of Kelly et al. [2]. An unusual feature in Fig. 13 is that with the alloy C, after 5 cycles, the peak current output is higher than that obtained with the uncycled case. This is probably due to the fact that the initial few cycles help to improve the porosity of the PbO_2 matrix. However, with the alloy E although the peak current output, and

Fig. 12. ln i vs $t^{-0.5}$ for falling part in Fig. 7 for cycled (20 cycles) alloy C based porous electrode.
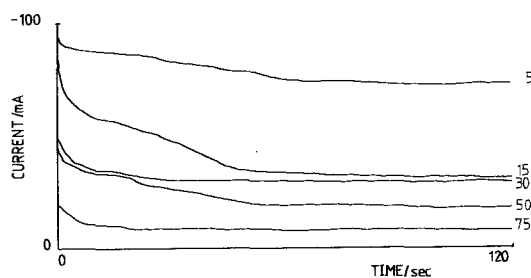

Fig. 14. As in Fig. 13, but for alloy E based porous electrode following a series of cycles.
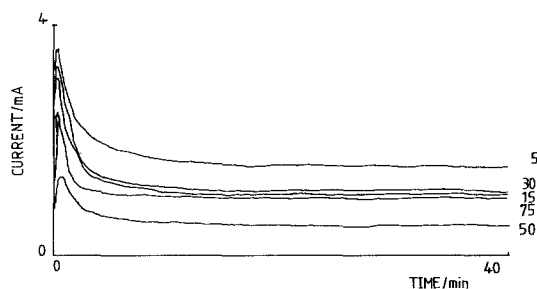
Fig. 15. Potentiostatic pulse experiments from 700 to 1240 mV (details as in Fig. 13) following a complete discharge.
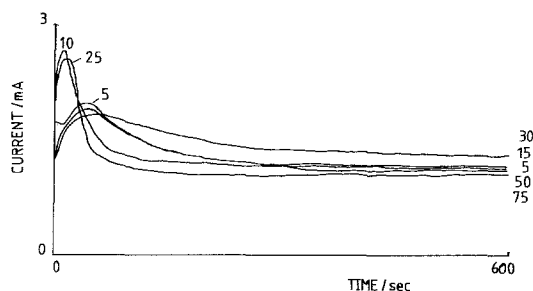

Fig. 16. Potentiostatic pulse experiments from 700 to 1240 mV (details as in Fig. 14) following a complete discharge.

hence charge, decreases with number of cycles as would be expected the uncycled 'positive' discharges most efficiently. Thus it seems quite significant that for a Pb–Sb electrode, a few preparatory cycles before a potentiostatic reduction pulse can increase the peak current output quite considerably, whereas with the Pb–Sn–Ca case, cycling beforehand has no significant effect.

Figs. 15 and 16 show the current–time responses for alloys C and E electrodes respectively after they had been subjected to a series of cycles, fully discharged by a potentiostatic reduction pulse, as in the case for Figs. 13 and 14, and finally oxidized back into the PbO$_2$ region. As can be seen there is no significant difference between the Pb–Sb and Pb–Sn–Ca positives.

We used again the Least Squares Fit method to match the falling parts of the transients in Figs. 13–16 but none of them followed an established current–time relationship for electrocrystallization reactions. However, after a potentiostatic oxidation pulse, with both electrodes, all the different preparatory cycle cases gave an i vs $t^{-1/2}$ relationship. It seems that only after sufficient cycles had been given is the porous matrix transformed into an extensively uniform phase.

4. Conclusions

Although the porous nature of the electrode results in a lack of control of the surface (and solution) pre-electrode condition of these experiments certain tentative conclusions can be drawn about the behaviour of the electrodes in our experimental conditions. These conditions are equivalent to high rates of operation (and recharge) of

the order of the minute rate. It should be recognized that these conclusions may not apply to other modes of operation.

(a) The uncycled pasted Pb–Sn–Ca electrodes discharge at a faster rate than the Pb–Sb electrodes

(b) All the electrodes accept charge very slowly after a complete discharge

(c) Initial cycling for the Pb–Sb positive results in a higher peak current output

(d) As the number of cycles increase, the peak current output of the electrodes, after a reductive pulse, decrease

(e) The imbalance between the charge output and input for the high rate potentiostatic cycling of lead acid cells clearly indicates the need for periodic galvanostatic conditioning charges

Acknowledgements

References

[1]   P. J. Mitchell, PhD thesis, Loughborough University (1983).
[2]   S. Kelly, N. A. Hampson and K. Peters, *J. Appl. Electrochem.* 11 (1981) 595.
[3]   J. Burbank, A. C. Simon and E. Willihnganz, *Adv. Electrochem. Electrochem. Eng.* 8 (1971) 157.
[4]   J. A. Bialacki, N. A. Hampson and K. Julian, *Surf. Technol.* 19 (1983) 347.
[5]   H. R. Thirsk and J. A. Harrison, 'A Guide to the study of Electrode Kinetics' (Academic Press, London and New York, 1972) p. 115.
[6]   J. L. Dawson, M. E. Rana, B. Munasiri and J. McWhinnie, 'Power Sources', 7, edited by J. Thompson (Academic Press Inc., New York, 1979) p. 1–15.